CHEMICAL ENGINEERING TRANSACTIONS
VOL. 109, 2024
A publication of AIDIC
The Italian Association of Chemical Engineering
Online at www.cetjournal.it
Guest Editors: Leonardo Tognotti, Rubens Maciel Filho, Viatcheslav Kafarov

ISBN 979-12-81206-09-0; **ISSN** 2283-9216
DOI: 10.3303/CET24109104

A New Viscosity Model for Non–Newtonian Fluids : Part I – Physical Characteristics of Its Mathematical Description

Tupthai Seethao*, Apinan Namkanisorn, Santi Wattananusorn

Department of Chemical Engineering, School of Engineering, King Mongkut's Institute of Technology Ladkrabang, Bangkok 10520, Thailand
tupthai.seethao@gmail.com

This research introduces a numerical approach for constructing a viscosity model, utilizing the power law model to illustrate the behavior of shear–thinning fluids in relation to fluid flow parameters. The developed viscosity model was integrated into a Computational Fluid Dynamics (CFD) tool and its performance was assessed by comparing predictions with experimental data from literature, as well as with various viscosity models such as power law, Sisko, Cross power law, and Bird–Carreau viscosity models. The results, along with the additional correlation obtained from a 100:1 planar channel flow simulation, demonstrated stability and efficiency.

1. Introduction

Non–Newtonian fluids are frequently encountered in various aspects of our daily lives, including personal care and cosmetic products, lubricating oils, polymer melts, and even the blood in our bodies, among others. The distinctive characteristic of these fluids is their viscosity, which changes in response to applied shear rate or shear stress. This behavior significantly influences processing operations and transportation in numerous applications, often serving as a pivotal factor in production efficiency and the final product's quality. Therefore, a comprehensive understanding of these intricate fluid properties is essential and holds fundamental importance in industrial sectors. Numerous studies in the literature focus on experimental and/or numerical analyses of non–Newtonian characteristics and fluid flows. These studies provide insights into the properties of fluids, which are influenced by shear rate and can be effectively described using various rheological models. One of the widely employed simplified models in specific types of research is the Ostwald–de Waele's relation (Ostwald, 1929), also known as the power law model. It is important to note that the power law model has limitations, specifically being valid over only a limited range of shear rates. Consequently, alternative models have been developed to address this limitation and provide accurate representations of fluid behavior across the entire range of shear rates such as Carreau–Yasuda model (Yasuda et al., 1981), Herschel–Bulkley model (Herschel and Bulkley, 1926), Bingham model (Bingham, 1922), among others. Despite extensive modeling of non–Newtonian phenomena, a clear explanation for the evolution of viscosity, considering flow characteristics (n, K, and $\dot{\gamma}$), from the initial stages through a vast range of the flow shear rate remains elusive. In light of this situation, modifying the viscosity model for non–Newtonian fluids, with a particular emphasis on shear–thinning behavior, emerges as a pertinent issue. Such modification holds the potential to elucidate the true nature of this fluid characteristic, offering a more accurate depiction of its behavior. This is the first of a set of papers aiming to develop a viscosity model for non–Newtonian fluids, specifically focusing on shear–thinning fluids. The proposed numerical methodology is based on the power law model. Leveraging advancements in computational power, the model's performance was rigorously assessed by comparing its predictions with both experimental and numerical data drawn from existing literature. The evaluation is carried out within the context of analyzing a 100:1 planar channel flow, employing OpenFOAM® for Computational Fluid Dynamics (CFD).

2. Methodology

This section presents the mathematical formulation and the fundamental concepts associated with the newly developed viscosity model.

Paper Received: 22 February 2024 ; Revised: 11 March 2024; Accepted: 18 May 2024
Please cite this article as: Seethao T., Namkanisorn A., Wattananusorn S., 2024, A New Viscosity Model for Non–newtonian Fluids : Part I – Physical Characteristics of Its Mathematical Description, Chemical Engineering Transactions, 109, 619-624 DOI:10.3303/CET24109104

2.1 Governing equations

The internal flow of non–Newtonian fluids, assumed to be isothermal and incompressible, is carried out with the mass conservation (continuity):

$$\nabla \cdot (\boldsymbol{u}) = 0 \tag{1}$$

and momentum conservation:

$$\frac{\partial(\rho \boldsymbol{u})}{\partial t} + \nabla \cdot (\rho \boldsymbol{u}\boldsymbol{u}) = -\nabla p + \nabla \cdot \boldsymbol{\tau} \tag{2}$$

in the above equations ρ is the density of the fluid, $\boldsymbol{u}$ is the velocity vector, p is the pressure, and $\boldsymbol{\tau}$ is the stress tensor or shear stress which is defined by

$$\boldsymbol{\tau} = 2\eta \mathbf{D} \tag{3}$$

where η is the dynamic viscosity of fluid and $\mathbf{D}$ is the symmetric rate of strain tensor given by

$$\mathbf{D} = \frac{1}{2}[\, \nabla \boldsymbol{u} + (\nabla \boldsymbol{u})^{\mathrm{T}} \,]. \tag{4}$$

The expression for $\boldsymbol{\tau}$ relies on inelastic non–Newtonian constitutive models, primarily characterized by viscosity and yield stress models. Table 1 displays commonly used viscosity models for non–Newtonian behavior, all of which are well–established and widely employed in the literature. Further details on these models and their parameters are available in numerous rheology publications.

Table 1: Commonly used viscosity models for non–Newtonian behavior.

Model name	Equation
Power law (Ostwald–de Waele relation)	$\eta = K\dot{\gamma}^{n-1}$
Sisko (Sisko, 1958)	$\eta = K\dot{\gamma}^{n-1} + \eta_\infty$
Cross power law (Cross, 1965)	$\eta = \eta_\infty + \left[\frac{(\eta_0 - \eta_\infty)}{1 + (m\dot{\gamma})^n}\right]$
Bird–Carreau (Bird and Carreau, 1968)	$\eta = \eta_\infty + (\eta_0 - \eta_\infty)[1 + (k\dot{\gamma})^2]^{\frac{(n-1)}{2}}$

2.2 Modification of viscosity model

Shear–thinning or pseudo–plastic fluids, characterized by a decrease in viscosity with increasing shear stress, represent the most common type of non–Newtonian behavior. The primary focus of developing the viscosity model in this study was centered around a range of power law numbers (n) that induce shear–thinning behavior. This can be obtained by starting from the relationship between shear rate and the fluid's viscosity at the onset of flow can be expressed as $\dot{\gamma} \to 0 : \eta \to \mu_0$ and when the flow reaches a high shear rate $\dot{\gamma} \to \infty : \eta \to \mu_\infty$. An infinite viscosity (μ_∞) can be related to the initial viscosity (μ_0) via the relation:

$$\mu_\infty = \frac{K^* \mu_0}{1 + K^*} \tag{5}$$

where K^* is called the modified consistency index of K in a sense of the path function of μ_0 as

$$K^* = \left(\frac{K}{\mu_0} - \theta\lambda^{n-1}\right)\dot{\gamma}^{n-1} \tag{6}$$

where λ is a time constant with θ being its scale factor. Then a new dynamic viscosity is now proposed by

$$\eta(\dot{\gamma}) = \frac{\mu_0}{1 + \left[\frac{1}{K^* + (\lambda|\dot{\gamma}|)^{n-1}}\right]}. \tag{7}$$

Due to the lower limit of Newtonian fluids, the parameter Ω is also required and Eq (6) finally becomes

$$\eta(\dot{\gamma}) = \frac{\Omega\, \mu_0}{1 + \left[\frac{1}{K^* + (\lambda|\dot{\gamma}|)^{n-1}}\right]} \tag{8}$$

where

$$\Omega \equiv \frac{K^* + 2}{K^* + 1}.$$

2.3 Geometry and flow conditions

To provide the fully developed length and the required flow rates for the entire study, a 2D planar channel with an aspect ratio of 100:1 was selected as the test geometry (Figure 1). A uniform velocity " *U* " is assigned at the entrance, with the absence of all other variables. Zero axial gradients are applied to all variables at the exit, except for the pressure, which is set to zero. At the wall, the no–slip boundary condition is used, along with symmetry at the centerline of the domain.

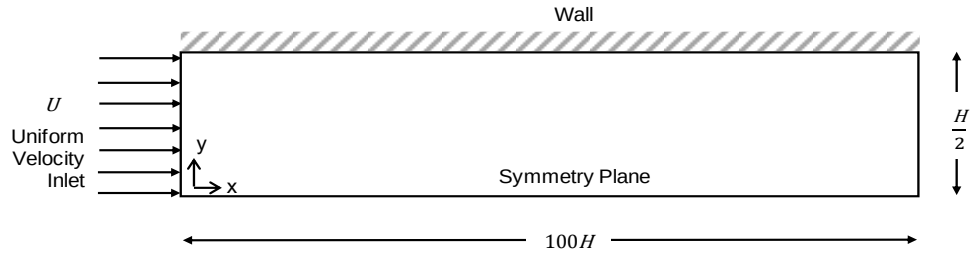

Figure 1: Schematic of computational domain and boundary conditions.

The system was discretized using the finite volume method. The coupling of pressure and velocity was achieved through the implementation of SIMPLE (Semi–Implicit Method for Pressure–Linked Equations), as proposed by Patankar (1972). The discretization of the different terms was made using the 2nd–order accurate scheme, the usual central differences scheme for the diffusion term and the bounded LUDS scheme for the momentum advective term, respectively. The observed scaled residuals for the solution approached an asymptotic value of 10^{-6} for both pressure and velocity. A series of preliminary calculations for mesh independent analysis were carried out using a Newtonian fluid at an intermediate generalized Reynolds number ($\mathrm{Re}_{\mathrm{gen}}$ = 10.33),

$$\mathrm{Re}_{\mathrm{gen}} = (8)^{1-n}\frac{\rho {D_h}^n U^{2-n}}{K}\left(\frac{n}{a+bn}\right)^n \tag{9}$$

Here, D_h represents the hydraulic diameter, U is the imposed average velocity, and a and b are geometric parameters characterizing the cross–section of the duct as defined by Kozicki et al (1966). Three hexahedral meshes with resolutions of 600 × 40 (*Mesh 1*), 1200 × 80 (*Mesh 2*), and 2400 × 160 (*Mesh 3*) were employed to demonstrate suitable mesh density and to investigate the accuracy of the simulations. A non–uniform cell size distribution was applied near the channel wall, which is a high gradient region. Additionally, for a quantitative comparison among these results, a relative error (E_r) was defined as follows

$$E_r = \frac{\left|X_i - X_{ref}\right|}{X_{ref}}. \tag{10}$$

Where X_i is the value of the considered variable at a specific mesh point, and X_{ref} is the corresponding analytical value. X_{ref} for centerline velocity at the outlet (U_{CV}) and pressure drop (Δp) were referred from the theory (Kundu et al., 2016). For the development length (l_D), the axial distance required for the centerline velocity to reach 99% of its fully developed value, X_{ref} was determined using Richardson's extrapolation. The values of E_r for each parameter are shown in Table 2. For all observed variables, the values of E_r for *Mesh 2* were lower than 0.1 % suggesting that this mesh establishes the desired accuracy with less computational time than *Mesh 3*. Thus, *Mesh 2* was used in all remaining tests discussed in the next sections.

Table 2: Mesh characteristics and relative error of interested parameter.

Mesh	Nx	Ny	NC	l_D/H	E_r		
					U_{CV} (outlet)	Δp	l_D
1	600	40	24,000	0.85	3.33×10^{-4}	4.83×10^{-4}	0.11
2	1,200	80	96,000	0.82	4.73×10^{-4}	8.33×10^{-6}	0.08
3	2,400	160	384,000	0.77	2.67×10^{-4}	5.00×10^{-4}	0.02

3. Results and discussion

The results related to the various stages of evaluating the newly adapted viscosity model are presented in the following sections including: (I) comparing the predictions of the developed model with experimental results from the literature, and (II) assessing the apparent viscosity from each constitutive model.

3.1 Comparison between simulation and experimental data

To validate the predictions, the simulated results obtained using this model are compared with experimental data presented by Ansari et al. (2020). The viscosity curves for 0.2 wt% and 0.4 wt% polyacrylamide solutions within the shear rate ($\dot{\gamma}$) range of 10 – 1000 s^{-1} are utilized to characterize the rheological properties of the validated fluids. By employing the summarized power law parameters available in the literature, the model demonstrates comparable results to the measured data, as illustrated in Figure 2.

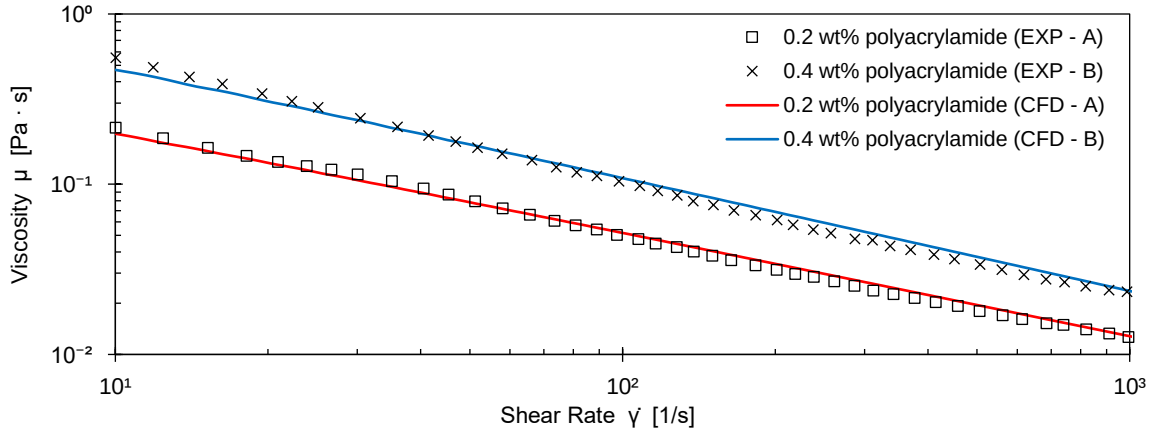

Figure 2: The viscosity of 0.2 wt% and 0.4 wt% polyacrylamide solutions at various shear rates.

With these same stated properties, simulated velocity profiles and measured velocity profiles can be compared. Figure 3 illustrates the velocity profiles of the validating fluid at $\mathrm{Re_{gen}}$= 1 and $\mathrm{Re_{gen}}$= 10, respectively. In all cases, good agreement with the experimental results was observed. The small differences can be attributed to the fact that the rheological characteristics of the fluid used in the present work were not entirely identical to those used in the experiment (Ansari et al., 2020).

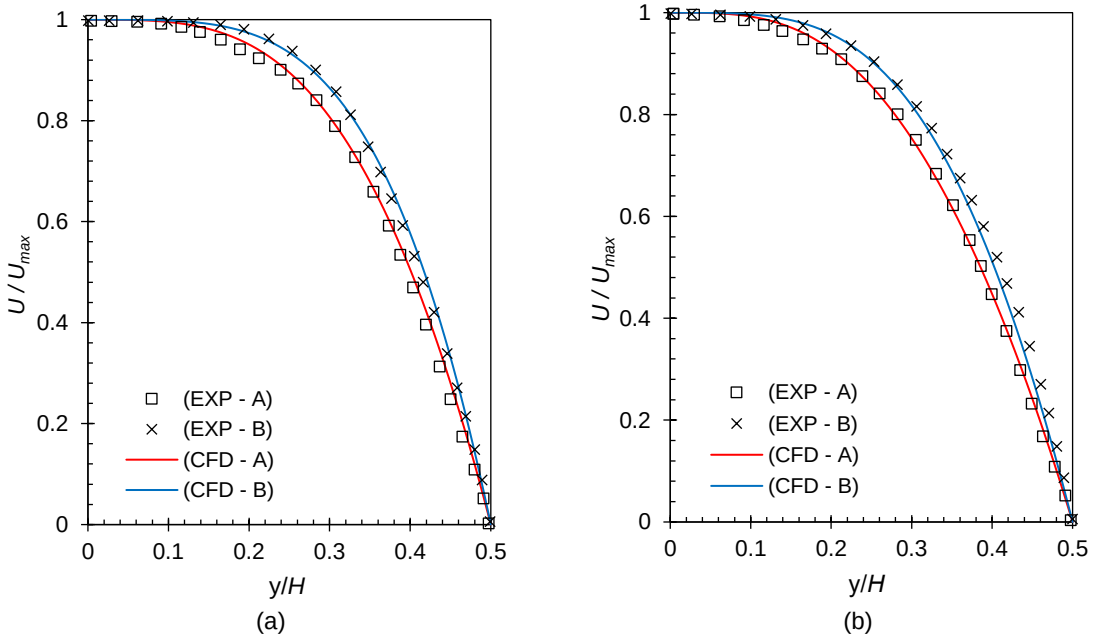

Figure 3: *The velocity profiles of the validating fluids at (a) Re_{gen}= 1 and (b) Re_{gen}= 10.*

3.2 The apparent viscosity from various viscosity models

In the realm of shear-thinning non–Newtonian fluids, numerous viscosity models find extensive use in diverse applications. Each model comes with its advantages and limitations. The selection of an appropriate model enhances usability, ensuring efficiency and satisfaction in terms of both quality and quantity. Consequently, a

thorough exploration of the capabilities of the recently developed viscosity model becomes imperative. Similarly, for the validation section, maintaining the same range of test fluid characteristics proves crucial. Literature data from Guillot and Dunand (1985) provided the measured data for Hydroxypropyl guar (HPG) using a coaxial cylinder viscometer. Moukhtari and Lecampion (2018) reproduced these experimental results and demonstrated them with various viscosity models, including power law, Carreau, and Ellis models. Simulations with different Reynolds numbers were conducted to establish a range of viscosity–shear rate relationships. Figure 4 illustrates the numerical predictions of viscosity for HPG fluid as a function of shear rate using different viscosity models. For comparison, experimental data are also included. From the results of simulated apparent viscosity, all viscosity models effectively predicted the shear–thinning characteristics of the interrelated testing fluid in the moderate shear rate zone, utilizing the rheological parameters outlined in Table 3. In comparison to the experimental data, the numerical results demonstrated a satisfactory qualitative agreement. Notably, the disparity among predictions from viscosity models started to converge and share the same value of fluid characteristics within a specific shear rate zone. However, beyond this zone, as the shear rate reached a certain threshold, the predictions began to vary again.

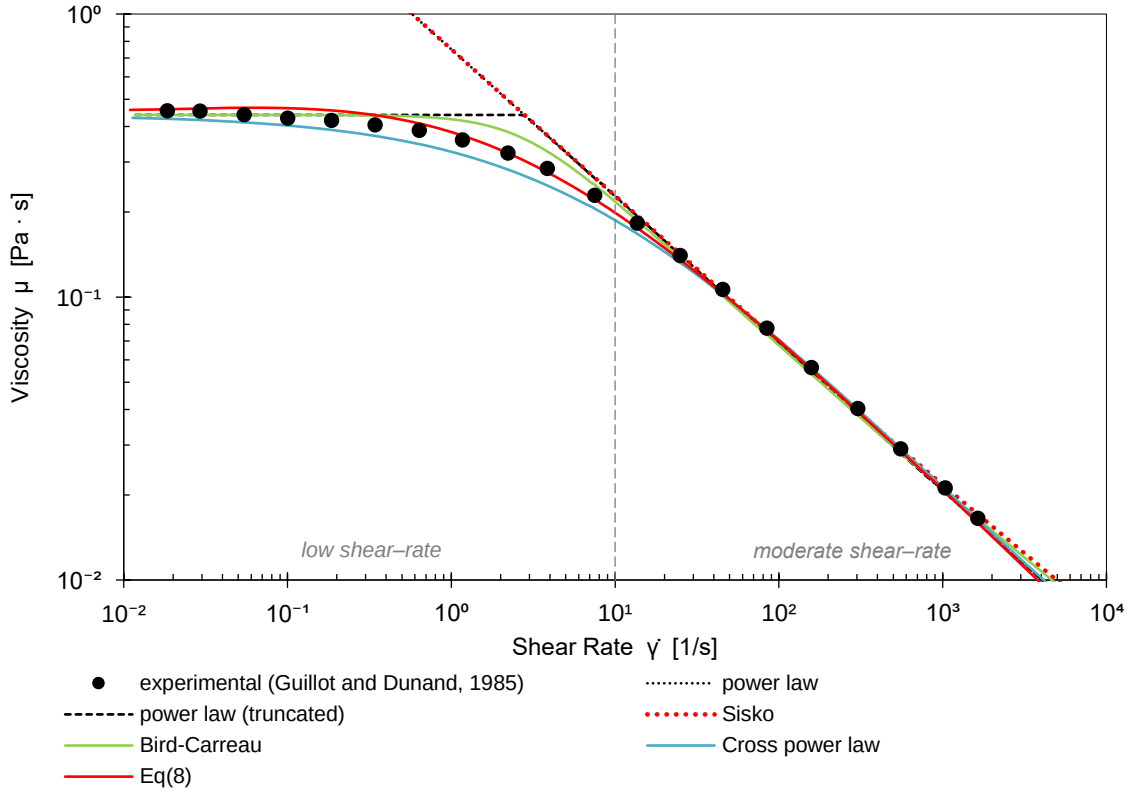

Figure 4: The relation curve of viscosity and shear rate of HPG fluid.

Table 3: Parameters of the HPG fluid for viscosity models depicted in Figure 4.

Model Name	Parameter	Value
Power law, Truncated power law, and Sisko	n	0.46
	K	0.75
Cross power law	n	0.59
	m	0.17
Bird–Carreau	n	0.48
	k	0.38
Proposed model – Eq(8)	n	0.44
	K	0.75
	λ	3.00
	θ	2.00
For all models (Except power law)	η_0	0.44
	η_∞	0.001

In low shear rate zone, the comparison of simulated results also reveals that the prediction from the proposed viscosity model qualitatively represent more consistent result with the experimental data among the other.

4. Conclusion

This study introduces a novel numerical methodology for developing a viscosity model based on the Ostwald–de Waele's relation or the power law model, aiming to capture the characteristics of shear–thinning non–Newtonian fluid through Computational Fluid Dynamics (CFD) simulations. Rigorous testing of the developed constitutive equation has demonstrated the stability and efficiency of the model constructed in this work. Comparisons between the predictions of the newly proposed viscosity model and experimental data obtained by Ansari et al. (2020) revealed the consistency and reliability of the developed tool. Additionally, a comprehensive comparison of the proposed model against experimental data (Guillot and Dunand, 1985) and various viscosity models was reported. The results exhibit good agreement with literature data in both low and moderate shear–rate zones, which being a generic range of the flow shear rate in several industrial processes and applications, affirming the success of the adopted methodology.

Nomenclature

ρ – density of fluid, kg/m^3
$\boldsymbol{u}$ – velocity vector, m^2/s
p – pressure, Pa
η – dynamic viscosity of fluid, kg/m s
$\boldsymbol{\tau}$ – stress tensor or shear stress, Pa
$\mathbf{D}$ – symmetric rate of strain tensor, 1/s
n – flow behavior index, -
K – flow consistency index, Pa s^n
$\dot{\gamma}$ – shear rate of the fluid's flow, 1/s
μ_0 – initial viscosity, kg/m s
μ_∞ – infinite viscosity, kg/m s
K^* – modified consistency index of K, -
λ – time constant for proposed viscosity model, s
θ – scale factor for time constant λ, -
$\mathrm{Re}_{\mathrm{gen}}$ – generalized Reynolds number, -
D_h – hydraulic diameter, m
U – imposed average velocity, m^2/s
a, b – geometric parameters characterizing the cross-section of the duct, -
E_r – relative error, -
m – time constant for Cross power law model, s
k – time constant for Bird–Carreau model, s

References

Ansari S., Ashker Ibney Rashid Md., Waghmare P.R., Nobes D.S., 2020, Measurement of the Flow Behavior Index of Newtonian and Shear–Thinning Fluids via Analysis of the Flow Velocity Characteristics in a Mini–Channel, *SN Applied Sciences*, 2:1787

Bingham E.C., 1922, Fluidity and Plasticity: Engineering, 5th Ed., McGraw Hill Book Company Inc., New York.

Bird R.B. and Carreau P.J., 1968, A Nonlinear Viscoelastic Model for Polymer Solutions and Melts–I, Vol 23, Chem. Eng. Sci, 427 – 434.

Cross M.M., 1965, Rheology of Non–Newtonian Fluids: A New Flow Equation for Pseudoplastic Systems, Vol 20(5), J. Colloid Science, 417 – 437.

Guillot D. and Dunand A., 1985, Rheological Characterization of Fracturing Fluids by Using Laser Anemometry, Vol 25(1), Soc. Petrol. Engng J., 39 – 45.

Herschel W.H. and Bulkley R., 1926, Konsistenzmessungen von Gummi–Benzollösungen, Vol 39 (4), Kolloid Zeitschrift, 291 – 300.

Kozichi W., Chou C.H. and Tiu C., 1966, Non–Newtonian Flow in Ducts of Arbitrary Cross–Sectional Shape, Vol 21, Chemical Engineering Science, 665 – 679.

Kundu, P.K., Cohen, I.M., Dowling, D.R., 2016, Fluid Mechanics, 6th Ed., Academic Press.

Moukhtari F.–E. and Lecampion B., 2018, A Semi–Infinite Hydraulic Fracture Driven by a Shear–Thinning Fluid, Vol 838, J. Fluid Mechanics, 573 – 605.

Ostwald W., 1929, Ueber die rechnerische Darstellung des Strukturgebietes der Viskosität, Vol 47 (2), Kolloid–Zeitschrift, 176 – 187.

Patankar S.V. and Spalding D.B., 1972, A Calculation Procedure for Heat, Mass and Momentum Transfer in Three–Dimensional Parabolic Flows, Vol 115, Int. J. Heat and Mass Transfer, 1787 – 1803.

Roumpea E., Chinaud M. and Angeli P., 2017, Experimental Investigations of Non–Newtonian / Newtonian Liquid–Liquid Flows in Microchannels, Vol 63, AIChE J., 3599 – 3609.

Sisko, A.W. 1958, The Flow of Lubricating Greases, Vol 50 (12), Industrial and engineering chemistry, 17898 – 1792.

Yasuda K., Armstrong R.C. and Cohen R.E., 1981, Shear Flow Properties of Concentrated Solutions of Linear and Star Branched Polystyrenes, Vol 20, Rheologica Acta, 163 – 178.